Solution Conformation of a Synthetic Fragment of Human Pituitary Growth Hormone. Two-Dimensional NMR of an α-Helical Dimer†

Vikram Roongta,‡ Robert Powers,‡ Claude Jones,‡ Michael J. Beakage,§ James E. Shields,§ and David G. Gorenstein*,‡

Department of Chemistry, Purdue University, West Lafayette, Indiana 47907, and Lilly Research Laboratory, Eli Lilly and Company, Indianapolis, Indiana 46285

Received June 1, 1988; Revised Manuscript Received September 23, 1988

ABSTRACT: Circular dichroism and two-dimensional NMR spectra indicate that a peptide fragment consisting of the first 28 residues from the N-terminus of human growth hormone (hGH 1–28) has considerable α-helical structure. The peptide, (1) H-Phe-Pro-Thr-Ile-Pro-Leu-Ser-Arg-Leu-Phe-Asp-Asn-Ala-Met-Leu-Arg-Ala-His-Arg-Leu-His-Gln-Leu-Ala-Phe-Asp-Thr-Tyr-OH (28), was synthesized on an automated peptide synthesizer using the Merrifield solid-phase method. The peptide can be modeled as an amphiphilic helix, and the unusual stability of the α-helix in aqueous solution is suggested to be attributable to formation of a dimer of α-helices. Most of the ^{1}H NMR signals were assigned through pure absorption phase COSY/NOESY and single- and double-relay COSY 2D NMR spectra by using the sequential assignment methodology. The NOEs were large and negative, suggesting that the peptide was not a random coil and that it existed in solution primarily as a large, fairly rigid macromolecule, consistent with the dimer structure. A network of $N_\alpha H_i$–$N_\alpha H_{i+1}$ NOESY crosspeaks is observed from residues 13 to 18 as are several other crosspeaks which indicate that the peptide has considerable α-helical structure between residues 8 and 24. In addition, gel filtration of the peptide is consistent with a dimer structure, presumably involving packing of the two hydrophobic faces of the amphiphilic α-helices.

Human pituitary growth hormone (hGH) (Li, 1982) is a protein of 191 amino acids, molecular weight about 22 100, which until recently was only available by extraction of cadaver pituitaries. It exhibits many different growth stimulatory activities in mammals, but its precise mode of action remains somewhat unclear. While the crystal structure of hGH is not known, the broad outline of its tertiary structure is likely similar to that of a genetically engineered variant of porcine growth hormone. An X-ray crystallographic study of this growth hormone has recently been published (Abdel-Maguid et al., 1987).

While solution NMR methods have been able to provide detailed structures of a number of proteins, these two-dimensional NMR methods unfortunately are not yet capable of providing three-dimensional structures of proteins the size of native hGH. However, as shown by recent work on a 56-residue fragment of lac repressor, it is possible to study the structure of a fragment of the native protein that we hope retains the elements of the native structure (Kaptein et al., 1985).

Many medium-length peptides have been subjected to conformational investigations. For instance, glucagon is well-known to have a concentration-dependent solution conformation (Korn & Ottensmeyer, 1983) that seems to approach the known crystal conformation (Sasaki et al., 1975) as concentration increases. Studies on atrial natriuretic hormone have indicated that this peptide lacks a well-defined solution conformation (Theriault et al., 1987). A recent ^{1}H 2D NMR study of fragment 96–133 of the related bovine growth hormone (bGH) revealed that a portion of the peptide fragment (residues 100–110) formed a stable Ω-loop in aqueous solution (Gooley et al., 1988). Other examples of stable reverse turns have been noted (Dyson et al., 1985). More recently, several examples of small peptides forming α-helical structures have been noted (Ihara et al., 1982; Kim & Baldwin, 1984; Shoemaker et al., 1987). In 30% trifluoroethanol the 96–133 fragment of bGH forms an α-helix spanning residues 106–128 (Gooley & MacKenzie, 1988). Apparently, the α-helix spanning residues 120–125 is also present in a fully aqueous medium at room temperature. Indeed, the Zimm–Bragg theory (Zimm & Bragg, 1959) would suggest that peptides shorter than 20 residues should not form much α-helical structure in aqueous solution. It appears, however, that either lower temperatures or addition of solvents such as trifluoroethanol or methanol are required to stabilize these α-helical structures (Bazzo et al., 1988).

In general, most small linear peptides exhibit little stable secondary structure in purely aqueous solution (Epand & Scheraga, 1968; Taniuchi & Anfinsen, 1969). Very little NOE data have been previously described that demonstrate a significant amount of α-helix in short linear peptides in purely aqueous solution. In this paper we describe the nearly complete ^{1}H NMR assignments of a chemically synthesized, 28-residue linear peptide as well as NMR and CD spectroscopy and gel filtration experiments that suggest that the short synthetic fragment of hGH forms an α-helix in purely aqueous solution at room temperature. We suggest that part of this unusual α-helix stability appears to be attributable to dimerization of these amphiphilic helices (Brems et al., 1986; Gooley & MacKenzie, 1988).

Materials and Methods

hGH Peptide Fragments. Peptide fragments of human growth hormone were synthesized on a Beckman Model 990B automated peptide synthesizer using the Merrifield solid-phase method (Merrifield, 1964; Stewart & Young, 1969). Frag-

† Supported by NIH (GM36281), the Purdue University Biochemical Magnetic Resonance Laboratory, which is supported by NIH (Grant RR01077 from the Biotechnology Resources Program of the Division of Research Resources), and NSF Biological Facilites Center on Biomolecular NMR, Structure and Design at Purdue (Grants BBS 8614177 and 8714258 from the Division of Biological Instrumentation).

‡ Purdue University.
§ Eli Lilly and Co.

0006-2960/89/0428-1048$01.50/0

ments consisting of the first 28 residues from the N-terminus of human growth hormone (hGH 1–28), (1) H-Phe-Pro-Thr-Ile-Pro-Leu-Ser-Arg-Leu-Phe-Asp-Asn-Ala-Met-Leu-Arg-Ala-His-Arg-Leu-His-Gln-Leu-Ala-Phe-Asp-Thr-Tyr-OH (28) (DeNoto et al., 1981), and additional hGH peptide fragments (25–45) (AFDTYQEFEEAYIPKEQKYSF) and (126–151) (RLEDGSPRTGQIFKQTYSKFDTNSHN) were synthesized as described below in detail for the (1–28) fragment.

N-t-BOC-*O*-(2,6-dichlorobenzyl)-L-tyrosyl-resin ester (15.0 g) prepared by the crown ether method (Roeske & Gesellchen, 1976) having a substitution level of 0.27 mmol/g was used in the Beckman automated peptide synthesizer, according to the protocols outlined in Table II of the supplementary material. The amino acid derivatives used in the synthesis are listed in Table I of the supplementary material. All residues were double coupled, and the resin was washed rigorously between steps using a shrink-swell procedure employing *tert*-butyl alcohol.

The completed peptidyl-resin was deblocked in liquid hydrogen fluoride. In the deblocking, 16.0 g of protected peptide resin was mixed with 21 mL of anisole and 21 mL of ethyl mercaptan. To this was added 250 mL of liquid hydrogen fluoride. This mixture was held 2 h at 0 °C, after which time the hydrogen fluoride was removed under vacuum. The residue was washed with ether and filtered, and the peptide was extracted with aqueous acetic acid.

Analytical reverse-phase HPLC of the crude material showed a pattern of peaks suggesting the presence of a slight degree of racemization of the two histidines, as well as partial oxidation of the single methionine to the sulfoxide.

Purification was effected by a series of column chromatography steps. The crude deblocked material was chromatographed on a column of Sephadex G-50 fine in dilute acetic acid. The desired material was pooled, lyophilized, and rechromatographed on a preparative reverse-phase HPLC system in 0.1 M ammonium formate, pH 4.25, and 33% acetonitrile. The major peak was collected and lyophilized until free of buffer salts.

Subsequent analytical reverse-phase HPLC indicated a purity of at least 85–90% of the material absorbing at 280 nm in the mean peak. A satisfactory amino acid analysis was also obtained. (Purity was also confirmed by the detailed ^{1}H NMR assignments and observation of only a few low-intensity signals integrating for less than 10–15% of the main peaks; see below.) This degree of impurities did not compromise the conformational analysis. Peptide fragments 25–45 and 126–151 were of comparable purity.

NMR. Pure absorption phase COSY/NOESY and single- and double-relay COSY 2D NMR spectra in H_2O and D_2O were obtained and analyzed following the sequential assignment methodology developed by Wüthrich and co-workers (Wüthrich, 1986). Peptide samples were prepared in purely aqueous solution, pH 3.0 (in D_2O, pH refers to the uncorrected pH meter reading), 7–8 mg/0.4 mL of sample volume. NMR spectra were recorded on a Nicolet 470-MHz NMR spectrometer and processed offline with Dennis Hare's FTNMR program on a Micro Vax II.

The pure absorption phase correlated spectra (COSY) were acquired by using a $(90°-t_1-90°-\text{acquire})_n$ pulse sequence with 2048 data points in the t_2 dimension and 1024 t_1 increments. A relaxation delay of 1.8 s was used between scans. For spectra recorded in 90% H_2O/10% D_2O, the large H_2O signal was suppressed by irradation during the delay, and a homospoil pulse of 20 ms with a recovery time of 20 ms was used.

Two-dimensional NOE (NOESY) spectra were acquired in the phase-sensitive mode by using the TPPI (Marion & Wüthrich, 1983) phase-cycling scheme using a $(90°-t_1-90°-\tau_m-90°-\text{acquire})_n$ pulse sequence. The spectra were acquired with 2048 points in the t_2 dimension and with 1024 t_1 increments. A mixing time (τ_m) of 300 ms was used with a relaxation delay of 1.8 s. For spectra recorded in 90% H_2O/10% D_2O, the H_2O signal was irradiated during the mixing time and the delay between scans. A homospoil pulse of 20 ms with a recovery time of 20 ms was applied just prior to the first 90° pulse. Both the COSY and phase-sensitive TPPI NOESY data were acquired with a spectral width of ±2127.65 Hz and treated with a Gaussian multiplication in both the t_1 and t_2 dimensions.

Single-relay coherence transfer (relayed COSY) spectra were acquired by using a $(90°-t_1-90°-\tau-180°-\tau-90°-\text{acquire})_n$ pulse sequence (Bax & Drobny, 1985; Eich et al., 1982). A τ value of 20 ms was chosen to optimize coherence transfer in the leucine spin system. The double-relay COSY spectra were similarly acquired with a pulse scheme involving an additional coherence transfer $-\tau-180°-\tau-90°-$ sequence inserted prior to acquisition. A τ value of 16 ms was used. For spectra recorded in 90% H_2O/10% D_2O, the large H_2O signal was suppressed by irradiation during a 1.6-s delay, and a homospoil pulse of 20 ms with a recovery time of 20 ms (single relay) or 25 ms (double relay) was used. The 512 t_1 increments of 2048 data point FIDS (t_2) were processed by using a Gaussian line-narrowing function in both dimensions in a similar manner as the COSY data.

Size exclusion gel chromatography was run on a 1.5 × 100 cm column of Sephadex G-75. The peptide (0.5–16 mg/mL) or protein standards in aqueous solution, pH 3, were applied to the column, and the effective molecular weight of the peptide was determined by interpolation from the calibration curve obtained in a separate run for the standards.

Circular dichroism spectra of peptide fragments 1–28, 25–45, and 126–151 were run on a Cary 61 or a JASCO Model J600 circular dichroism spectrometer, generally at 25 °C. The peptides were dissolved in either 0.01 M HCl, dilute HCl (pH 3.5), 0.03 M phosphate buffer (pH 5.5 or 7), or 0.021 M phosphate buffer (pH 7), and 30% trifluoroethanol. The CD spectra were obtained in a 0.05 cm path length cell. The concentration and temperature dependence to the CD spectra of peptide 1–28 was made in D_2O, pH 3.5, at concentrations of 0.5–16 mg/mL. Spectra were obtained in 0.01–0.05 cm path length cells and represent the computer average of five scans for each concentration.

Results and Discussion

NMR Assignments. Most of the ^{1}H NMR signals were assigned through pure absorption phase 2D NMR spectra in H_2O and D_2O using the sequential assignment methodology developed by Wüthrich and co-workers (Wüthrich, 1986). Significantly, the NOEs were large and negative, suggesting that the peptide was not a random coil and that a significant population of the peptide existed in solution as a large, fairly rigid macromolecule. Additional data supporting the non-random-coil structure for the peptide fragment derive from the chemical shifts of the molecule. The chemical shifts of many of the residues differ significantly from the "random" coil conformation chemical shifts (Wüthrich, 1986). These large conformation-dependent chemical shift perturbations can arise from H-bonding secondary structures.

The basic sequential assignment approach is to utilize both *J* coupling and dipolar coupling connectivities to first establish the various spin systems of the different amino acid residues

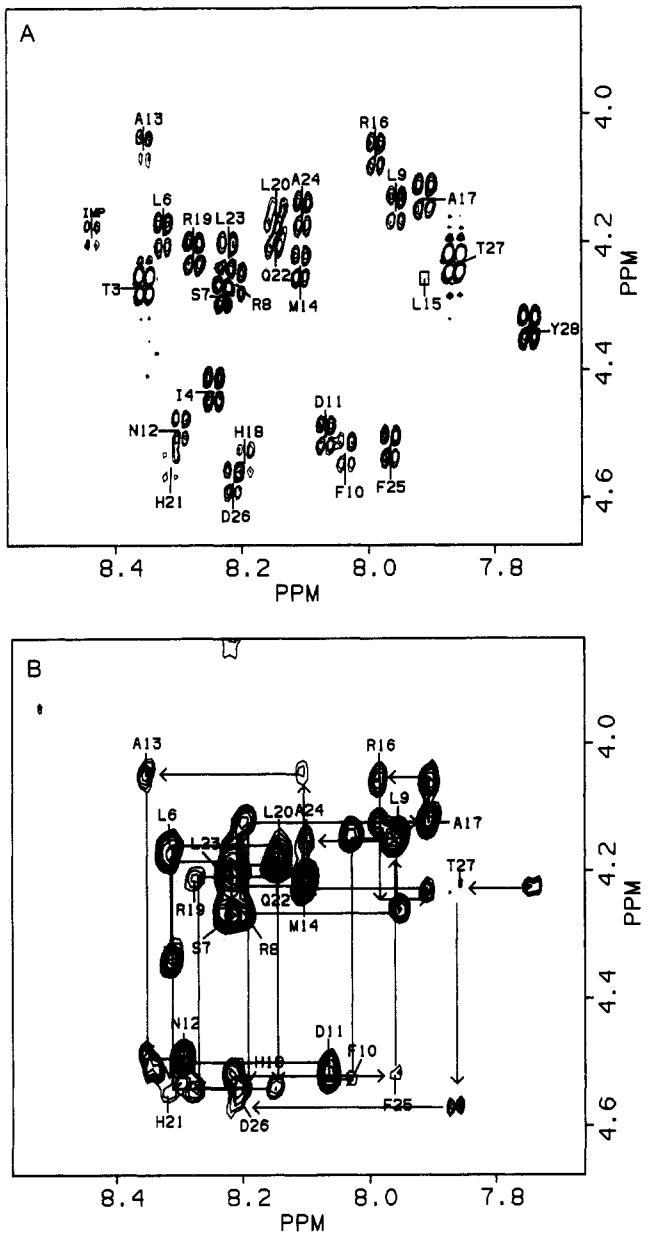

FIGURE 1: Pure absorption phase H_2O 2D COSY (A) and NOESY (B) spectra of the 1–28 N-terminal peptide fragment of human growth hormone in aqueous solution, pH 3.0, with expansion of the fingerprint region of the spectrum, showing the $C_\alpha H$–$N_\alpha H$ ^1H crosspeaks and sequential connectivity. Data were acquired on a Nicolet 470-MHz NMR spectrometer and processed offline with Dennis Hare's FTNMR program on a Micro Vax II.

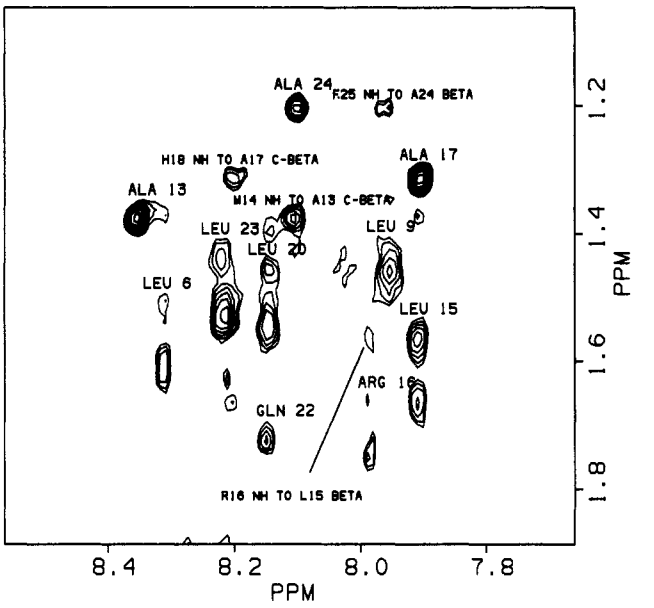

FIGURE 2: Pure absorption phase H_2O 2D NOESY spectra of the 1–28 N-terminal peptide fragment of hGH. Interresidue crosspeaks between $C_\beta H_i$–$N_\alpha H_{i+1}$ protons and intraresidue crosspeaks in the leucine and alanine spin systems are identified.

in the peptide. We predominantly relied upon single- and double-relay COSY 2D NMR spectra in H_2O to establish the spin system connectivity within each residue. These spectra allow connectivity between the $N_\alpha H_i$, $C_\alpha H_i$, $C_\beta H_i$, and $C_\gamma H_i$ protons (Wüthrich, 1986). Examples of the pure absorption phase D_2O COSY, single- and double-relay H_2O COSY spectra in the aliphatic and NH and C_α region are shown in Figures 1–3 of the supplementary material.

Thus, in the COSY spectrum (Figure 1 of the supplementary material) we observe the expected five crosspeaks connecting the methyl groups of alanines and threonines to their respective C_α or C_β methine protons. Only three of the five methyl groups appear in the H_2O single-relay COSY spectrum (Figure 2 of the supplementary material) that connects the β-methyl groups to the amide NH of the alanines only. In a double-relay COSY spectrum (Figure 3 of the supplementary material) we can extend the coherence transfer out further along the side chain and pick up two additional crosspeaks between the threonine γ-methyl and the amide NH. In this way we have been able to identify the three alanine and two threonine spin systems in the peptide fragment. The leucine NH to C_β and C_γ proton crosspeaks can also be identified in the relay spectra. Most of the spin systems were identified in this manner.

2D NMR Methodology. Sequential Assignment. The next stage of assignments is to establish connectivities across the peptide bond and to utilize the known primary sequence and the through-space connectivity provided by 2D NOESY to assign a spin system to a particular residue. There is no J (and hence COSY) connectivity between $C_\alpha H_i$ and $N_\alpha H_{i+1}$ protons and between $C_\beta H_i$ and $N_\alpha H_{i+1}$ protons; however, in most reasonable conformations of the polypeptide (particularly in α-helices), these protons are often within 4 Å of each other and hence show NOESY crosspeaks. As shown in Figure 1, one of the crucial regions of the 2D NOESY and COSY spectra is the fingerprint $N_\alpha H$–$C_\alpha H$ region. In this fingerprint region (Figure 1), we see both NOESY and COSY crosspeaks in general between intraresidue $C_\alpha H_i$ and $N_\alpha H_i$ since both J and dipolar couplings exist between these protons. We also observe only NOESY crosspeaks between the $C_\alpha H_i$ and $N_\alpha H_{i+1}$ residues. By the sequential connectivity between the COSY and NOESY crosspeaks in Figure 1 and various other spectra not shown, we have assigned almost all of the proton signals of the fragment. The $C_\beta H_i$–$N_\alpha H_{i+1}$–H_2O NOESY crosspeaks were particularly helpful in confirming the sequential assignments (cf. Figure 2). The proton assignments are listed in Table I.

Secondary Structure. The next stage in the structural analysis is to determine any elements of secondary structure of the peptide by using additional NOESY information. Thus, if an α-helix is present, we should observe several NOESY crosspeaks corresponding to short distances imposed by the secondary structure of the protein. In a regular α-helix the distance between the $C_\alpha H_i$ and the $N_\alpha H_{i+1}$ protons is near the maximum possible separation of 3.5 Å, while the $N_\alpha H_i$–$N_\alpha H_{i+1}$ distance is 2.8 Å. In an extended conformation, the relative distances are just the opposite (Wüthrich, 1986). Thus, the NH–NH NOESY region (Figure 3) is particularly

Table I: ^{1}H NMR Assignments of the 28 Amino Acid N-Terminal Fragment of Human Growth Hormone

residue	NH	α-H	β-H	others
Phe 1		4.52	3.05, 3.31	2, 6 H 7.14
				3, 5 H 7.23
				4 H 7.35
Pro 2		4.56	1.84, 2.25	γ-CH_2 1.93
				δ-CH_3 3.37, 3.73
Thr 3	8.35	4.27	4.11	γ-CH_3 1.15
Ile 4	8.24	4.47	1.80	γ-CH_3 0.88
				γ-CH_2 1.56
				δ-CH_3 0.83
Pro 5		4.34	1.86, 2.23	γ-CH 1.95
				δ-CH_3 3.10, 3.57
Leu 6	8.32	4.18	1.66	γ-CH_2 1.56
				δ-CH_3 0.77
Ser 7	8.23	4.26	3.81, 3.88	
Arg 8	8.21	4.26	1.79, 1.73	γ-CH_2 1.71, 1.53–1.58
				δ-CH_2 3.10
Leu 9	7.95	4.15	1.49	γ-CH_2 1.39
				δ-CH_3 0.84
Phe 10	8.03	4.53	2.96, 3.12	2, 6 H 7.14
				3, 5 H 7.23
				4 H 7.35
Asp 11	8.06	4.50	2.67	
Asn 12	8.29	4.49	2.83	δ-NH_2 7.65
Ala 13	8.35	4.05	1.41	
Met 14	8.11	4.24	2.06	γ-CH_2 2.54, 2.40
				ε-CH_3 2.25
Leu 15	7.91	4.25	1.71	γ-CH 1.61
				δ-CH_3 0.82
Arg 16	7.98	4.06	1.82	γ-CH_2 1.71, 1.53–1.58
				δ-CH_2 3.10
Ala 17	7.91	4.13	1.36	
His 18	8.19	4.54	3.20, 3.28	2 H 8.32
				4 H 7.19
Arg 19	8.27	4.22	1.79, 1.80	γ-CH_2 2.05, 1.53–1.58
				δ-CH_2 3.10
Leu 20	8.14	4.15	1.58	γ-CH 1.50
				δ-CH_3 0.90
His 21	8.31	4.55	3.20, 3.28	2 H 8.32
				4 H 7.19
Gln 22	8.15	4.19	2.03	γ-CH_2 2.25
Leu 23	8.22	4.23	1.57	γ-CH 1.47
				δ-CH_3 0.85
Ala 24	8.10	4.16	1.25	
Phe 25	7.95	4.52	2.93, 3.11	2, 6 H 7.14
				3, 5 H 7.23
				4 H 7.35
Asp 26	8.21	4.57	2.61	
Thr 27	7.86	4.23	4.14	δ-CH_3 1.06
Tyr 28	7.74	4.33	2.80, 2.99	2, 6 H 7.04
				2, 5 H 6.73

informative. A striking network of crosspeaks is observed from residues 13 to 18 as are several other $N_\alpha H_i$–$N_\alpha H_{i+1}$ crosspeaks between residues 8/9 and 23/24. Additional support for an α-helical section between residues 8 and 24 is provided by the $C_\beta H_i$–$N_\alpha H_{i+1}$ connectivities (cf. Figure 2), where often these crosspeaks are more intense in α-helical regions (Hahn & Ruterjans, 1985). (Alternatively the $C_\beta H_i$–$N_\alpha H_{i+1}$ crosspeaks could arise from intermolecular NOEs between two stacked α-helices, although there are no additional data to support this interpretation.) We have indicated these secondary structure crosspeaks for the fragment on the helical map of Figure 4.

Finally, the three-bond coupling constant ($^3J_{C_\alpha H\text{-}N_\alpha H}$) is generally less than 5 Hz in regions of α-helix and >7 Hz in extended chains (Wüthrich, 1986). In those residues where the NH is clearly resolved in the 1D NMR spectrum, coupling constants $^3J_{C_\alpha H\text{-}N_\alpha H}$ = 4–5.5 are observed for residues 10, 11, 13–15, 17, and 24. $^3J_{C_\alpha H\text{-}N_\alpha H}$ values of 7.5 Hz are observed for residues 16, 27, and 28.

Although observation of $N_\alpha H_i$–$N_\alpha H_{i+1}$ and $C_\beta H_i$–$N_\alpha H_{i+1}$ connectivities and small $^3J_{C_\alpha H\text{-}N_\alpha H}$ is not definitive, these results

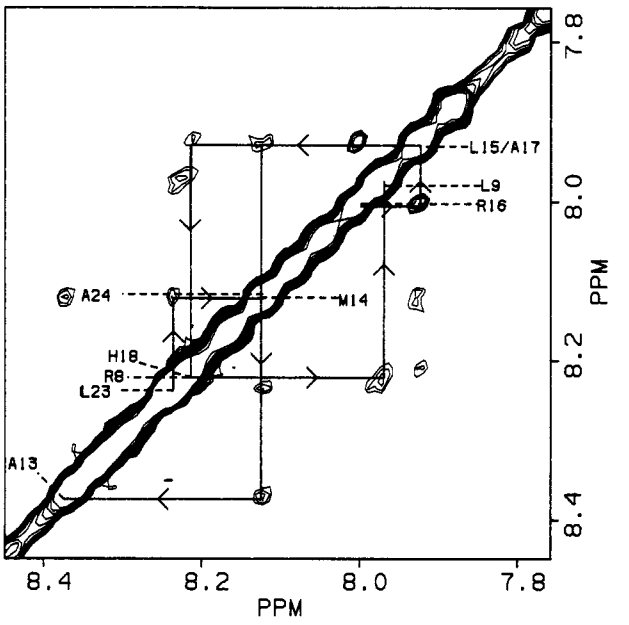

FIGURE 3: Amide NH region of the pure absorption phase NOESY spectrum of hGH 1–28. $N_\alpha H_i$–$N_\alpha H_{i+1}$ connectivities are noted between indicated residues, suggestive of α-helical character.

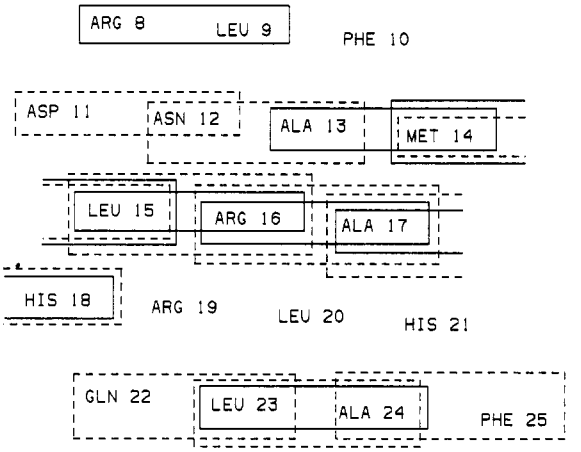

FIGURE 4: Peptide map of hGH fragment 1–28. $N_\alpha H_i$–$N_\alpha H_{i+1}$ NOESY connectivities are shown in solid outline boxes, and $C_\beta H_i$–$N_\alpha H_{i+1}$ NOESY connectivities are shown in dashed outline boxes.

suggest a significant degree of α-helix structure between residues 8 and 24. We emphasize that these spectra were run in water at room temperature in purely aqueous solution (with added α-helix stabilizing solvent trifluoroethanol we do see additional $N_\alpha H_i$–$N_\alpha H_{i+1}$ crosspeaks and all of these crosspeaks are significantly more intense under these conditions).

Prediction of secondary structure stability by Chou–Fasman analysis (Chou & Fasman, 1978) is consistent with stretches of α-helix between residues 9 and 15 (P_α = 1.17) and 17 and 25 (P_α = 1.24; overall P_α = 1.18 for residues 9–25). Generally, values of α-helix propensity (P_α) greater than 1.1 indicate a good probability that the sequence can form an α-helix. In addition, the nonpolar residues occur in triplets at relative positions 1–2–5 and 1–4–5. This clustering of nonpolar triplets is observed in amphiphilic helices in which the nonpolar residues cluster on one face of the α-helix and the hydrophilic residues are found on the opposite face (Schulz & Schirmer, 1979). Indeed, a helix map (Figure 4) of residues 8–24 of the primary sequence of hGH 1–28 conforms very nicely with an amphiphilic structure. The amphiphilic nature of the arrangement of the amino acids also appears to be a factor in α-helix stabilization (Ho & DeGrado, 1987).

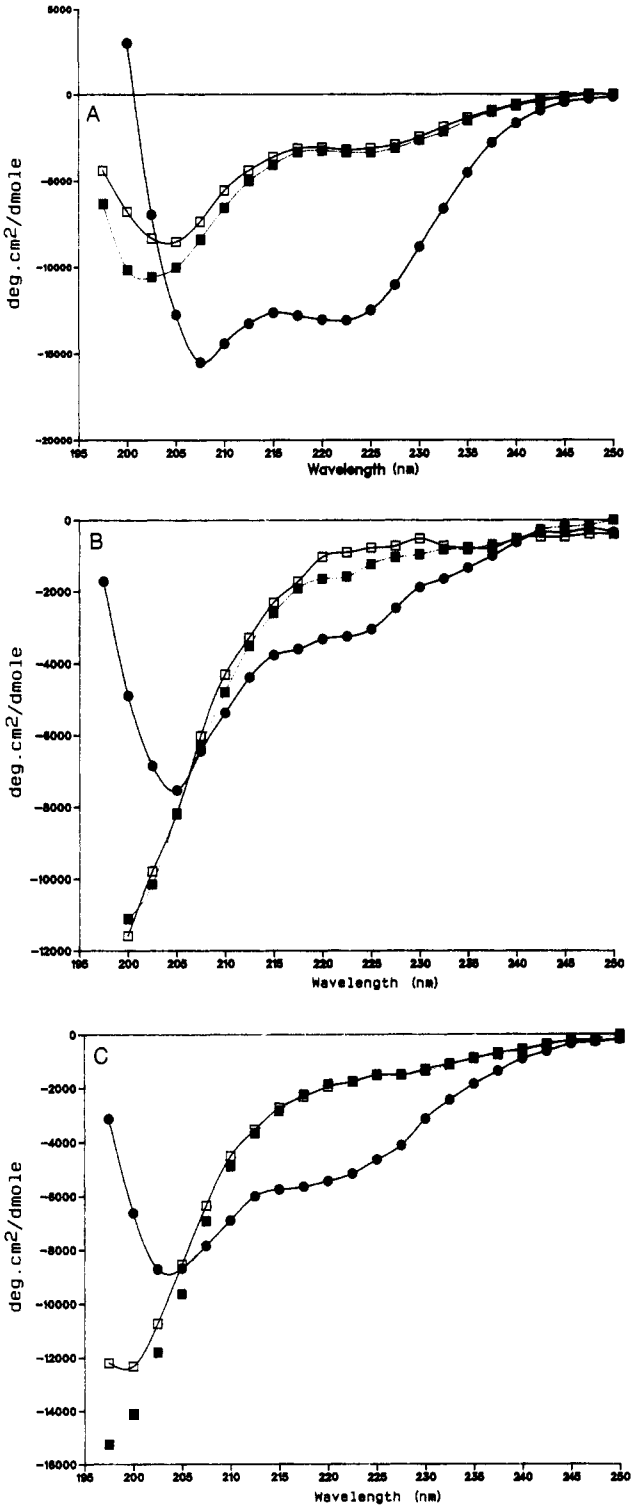

FIGURE 5: Circular dichroic spectra for hGH peptide fragment 1–28 (A), 25–45 (B), and 126–151 (C) at 25 °C, 0.01 M HCl (■), 0.03 M phosphate, pH 5.75 (for A), and pH 7.0 (for B and C) (□), 0.021 M phosphate, and 30% trifluoroethanol (●), concentration 0.25–0.37 mg/mL.

The circular dichroic spectra of peptide fragments 1–28, 25–45, and 126–151 are shown in Figure 5. The circular dichroic (CD) spectra of the three synthetic fragments of hGH indicate that only peptide 1–28 has significant α-helical character in aqueous solution. Thus, the ellipticity at 222 nm ($[\theta]_{222}$) for the hGH fragment 1–28 is ca. −4000 deg cm^2/dmol at 25 °C in aqueous solution, pH 3.5 (spectrum not shown; see Figure 5A for comparable conditions). As shown in parts B and C of Figure 5, no apparent peak is observed at $[\theta]_{222}$ for the peptide fragments 25–45 and 126–151. On the basis of the $[\theta]_{222}$ of −26 500 deg cm^2/dmol for 100% helix formation of a 13-residue C-peptide from ribonuclease (Shoemaker et al., 1987) and assuming that only residues 8–24 (17 residues out of 28; see below) of the hGH fragment 1–28 can form an α-helix, we estimate that the hGH fragment is ca. 23% α-helix between residues 8 and 24 at 25 °C and pH 3.5. The ellipticity increases to −14 000 at 222 nm in 30% trifluoroethanol (Figure 5A), suggesting that the α-helical content between residues 8 and 24 increases to nearly 90% under these conditions. Peptide fragments 25–45 and 126–151 show a much smaller increase in the ellipticity at 222 nm in 30% trifluoroethanol (Figure 5B,C). A computer fit of the CD spectra of peptide fragment 1–28 also indicates a comparable amount of α-helix content as estimated above (Yang et al., 1986).

The CD results provide an explanation for the relative weakness of the NH–NH NOESY crosspeaks. Only ~23% of the molecules in solution are suggested to have a significant stretch of α-helical structure between residues 8 and 24. In the presumed random-coil conformation for the remainder of the molecules, the NH_i–NH_{i+1} distances will on average be much longer than those found in the α-helix and contribute very little to the NH_i–NH_{i+1} crosspeak volumes. In trifluoroethanol, where the α-helix content of the peptide increases substantially, the number and intensities of the NH_i–NH_{i+1} crosspeaks increase significantly (data not shown).

Size Exclusion Gel Chromatography. The effective molecular weight of the hGH 1–28 peptide was determined by size exclusion gel chromatography on a Sephadex G-75 column. The elution volume of the peptide varied slightly depending upon the concentration of the applied sample (Figure 4 of the supplementary material). The calculated molecular weight, based upon the protein standards curve, varied between 4600 and 5900. This is 1.4–1.8 times the monomer molecular weight for the peptide (3345). The concentration dependence of the exclusion gel data as well as that of the CD data suggests that at higher concentrations (greater than ca. 4 mg/mL of the peptide) the structure appears to become more ordered. Thus, the mean residue ellipticity at 222 nm decreases from −3.3 to −3.7 between 0.39 and 10.4 mg/mL of peptide. Similarly, the mean residue ellipticity at 222 nm of a 1.17 mg/mL, pH 3.5, solution of peptide fragment 1–28 increases from −3.8 (at 10 °C) to −3.4 (at 40 °C). An unusual aspect of the gel exclusion data is that at higher peptide concentrations the effective molecular weight appears to decrease slightly. This could be attributable to the formation of a smaller, more compact structure (i.e., stacked α-helices) that migrates slower through the gel than the less compact, largely random-coil peptide present at lower concentrations. Of course at any concentration, all of these structures are present in rapid equilibration with each other.

Model for the hGH 1–28 α-Helix Dimer. The hydrodynamic behavior of the peptide on size exclusion chromatography is consistent with formation of a dimer aggregate in equilibrium with the monomer fragment. Such self-association has been observed in amphiphilic helices (Ho & DeGrado, 1987). This aggregation also explains the large and negative NOEs observed. The unusual stability of the α-helix in aqueous solution is thus likely attributable to the dimer structure. The dimer presumably arises from the interaction between the hydrophobic faces of two antiparallel amphiphilic α-helices. Calculation of helix–helix docking using the Richmond and Richards (1978) algorithm suggests that residues 13, 14, and 17 present optimal sites for docking of two class III α-helices.

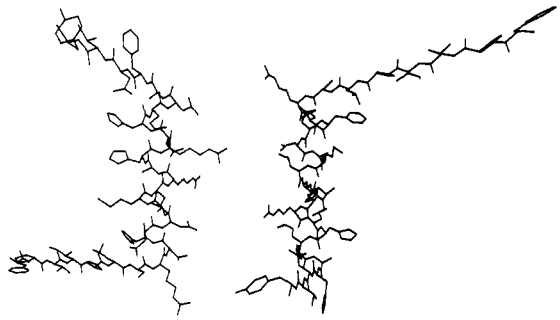

FIGURE 6: MIDAS model for a dimer of antiparallel α-helices between residues 8 and 24 for the hGH fragment, consistent with the NMR data and optimal docking near residues 13, 14, and 17.

We have utilized this information and the molecular modeling program MIDAS (Langridge & Ferrin, 1984) to model build on a Silicon Graphics Iris 3030 workstation a dimer of antiparallel α-helices between residues 8 and 24 for the hGH fragment consistent with the NMR data and optimal docking near residues 13, 14, and 17 (Figure 6). Using the AMBER (Weiner & Kollman, 1981) molecular mechanics energy minimization program, we first calculated a minimum energy structure for the α-helix monomer consistent with the NMR results. The model shown in Figure 6 represents a manual docking of two energy-minimized equivalent α-helices. There appear to be no unfavorable interactions, and the hGH sequence appears to be perfectly capable of forming a reasonable α-helix dimer between residues 8 and 24 (note two prolines, which would be helix breakers, are located at the N-terminus and indeed we do not see any NOESY crosspeaks indicative of any secondary structure in the first seven residues). The C-terminus has also been modeled as a random coil, consistent with the lack of any NOESY NH–NH crosspeaks in this region as well.

Conclusions. After our NMR study was completed, the X-ray structure of porcine growth hormone (pGH) appeared (Abdel-Maguid et al., 1987). There is considerable sequence homology between the two growth hormones, and the pGH is a four-helix bundle, with the N-terminus part of a long α-helix (residues 7–35). It is therefore potentially relevant that the above NMR and CD studies on the hGH fragment (residues 1–28) have indicated a remarkable ability of the peptide to form a stable amphiphilic α-helix in *purely* aqueous solution. In contrast, the CD data suggest that hGH peptide fragments 25–45 and 126–151 possess very little α-helix in either aqueous solution or even TFE solution. Very recently Gooley and MacKenzie (1988) have shown that residues 120–125 of a bovine growth hormone peptide fragment 96–133 also form a stable α-helix in purely aqueous solution and that in 30% TFE/70% H_2O the boundaries of this helix are residues 106–128. This stabilization is also attributed to hydrophobic interaction between two amphiphilic helices (Brems et al., 1986). Our N-terminal fragment (1–28) overlaps significantly with α-helix 1 of the bGH, and Gooley and MacKenzie's (1988) fragment 96–133 overlaps with helix 3 spanning residues 106–128 of the bGH. Peptide fragment 25–45 spans the C-terminus of helix 1 and a loop connecting helix 2 of bGH (Abdel-Maguid et al., 1987). Peptide fragment 126–151 spans the last few residues of the C-terminus of helix 3 and a loop connecting helix 4 of bGH (Abdel-Maguid et al., 1987). Of course, our observation of an α-helical dimer structure for the hGH peptide fragment 1–28 may have no bearing on the structure of the intact hGH protein. However, the four-helix bundle protein structure is stabilized by hydrophobic interactions between four amphiphilic helices. The tight interhelical association of the close-packed apolar residues on one face of the amphiphilic helix and the interdigitation between residues on neighboring helices is presumably responsible for this association (Chothia, 1984; Ho & DeGrado, 1987). Ho and DeGrado (1987) have recently demonstrated that a designed 16-residue amphiphilic α-helix appears to self-associate in solution to form a four-helix bundle protein. This cooperative tetramerization was predicted on the basis of secondary structure prediction rules (Chou & Fasman, 1978) and model building. It is thus quite likely that the amphiphilic α-helix in the hGH fragment is presumably part of a four-helix bundle protein consistent with the pGH X-ray structure.

As shown above, we can define the solution structure of a chemically synthesized peptide fragment by two-dimensional NMR methods using data acquired at only a single temperature and solvent composition. The double-relay COSY spectra and careful water suppression in the NOESY and COSY (H_2O) spectra were key components in this analysis. Significant NMR and analysis time can be saved if all of the assignments can be made on a sample run in a single solvent and at a single temperature. We also emphasize that these studies were conducted in purely aqueous solution at 25 °C, where it has generally been believed that little α-helical structure of a small peptide should be possible. This unusual stabilization of an α-helical structure in our hGH 1–28 fragment is likely attributable to formation of a dimer or even a more weakly associating four-helix bundle structure between the hydrophobic faces of the amphiphilic α-helix. Finally, the significant degree of α-helical structure for hGH fragment 1–28 and bGH fragment 96–133 (Gooley & MacKenzie, 1988) and the lack of defined secondary structure for hGH fragments 25–45 and 126–151 are entirely consistent with the X-ray structure of porcine growth hormone (Abdel-Maguid et al., 1987). At least in this protein, it thus appears to be possible to dissect the basic structural elements of the protein by analyzing the solution conformation of various peptide fragments.

ACKNOWLEDGMENTS

The contributions of R. Santini are much appreciated.

SUPPLEMENTARY MATERIAL AVAILABLE

Tables for peptide synthesis protocols and figures for 2D NMR of human growth hormone fragment 1–28 as well as a plot of CD and gel filtration data vs concentration (10 pages). Ordering information is given on any current masthead page.

REFERENCES

Abdel-Maguid, S. S., Shieh, H.-S., Smith, W. W., Dayringer, H. E., Violand, B. N., & Bentle, L. A. (1987) *Proc. Natl. Acad. Sci. U.S.A. 84*, 6434–6437.

Bax, A., & Drobny, G. (1985) *J. Magn. Reson. 61*, 306–320.

Bazzo, R., Tappin, M. J., Pastore, A., Harvey, T. S., Carver, J. A., & Campbell, I. D. (1988) *Eur. J. Biochem. 173*, 139–146.

Brems, D. N., Plaisted, S. M., Kauffman, E. W., & Havel, H. A. (1986) *Biochemistry 25*, 6539–6543.

Chothia, C. (1984) *Annu. Rev. Biochem. 53*, 537–572.

Chou, P. Y., & Fasman, G. D. (1978) *Adv. Enzymol. Relat. Areas Mol. Biol. 47*, 45–149.

DeNoto, F. M., Moore, D. D., & Goodman, H. M. (1981) *Nucleic Acids Res. 9*, 3719–3730.

Dyson, H. J., Cross, K. J., Houghten, R. A., Wilson, I. A., Wright, P. E., & Lerner, R. A. (1985) *Nature (London) 318*, 480–483.

Eich, G., Bodenhausen, G., & Ernst, R. R. (1982) *J. Am. Chem. Soc. 104*, 3731-3732.
Epand, R. M., & Scheraga, H. A. (1968) *Biochemistry 7*, 2864-2872.
Gooley, P. R., & MacKenzie, N. E. (1988) *Biochemistry 27*, 4032-4040.
Gooley, P. R., Plaisted, S. M., Brems, D. N., & MacKenzie, N. E. (1988) *Biochemistry 27*, 802-809.
Hahn, U., & Ruterjans, H. (1985) *Eur. J. Biochem. 152*, 481-491.
Ho, S. P., & DeGrado, W. F. (1987) *J. Am. Chem. Soc. 109*, 6751-6758.
Ihara, S., Ooi, T., & Takahashi, S. (1982) *Biopolymers 21*, 131-145.
Kaptein, R., Zuiderweg, E. R. P., Scheek, R. M., Boelens, R., & van Gunsteren, W. F. (1985) *J. Mol. Biol. 182*, 179-182.
Kim, P. S., & Baldwin, R. L. (1984) *Nature (London) 307*, 329-334.
Korn, A. P., & Ottensmeyer, F. P. (1983) *J. Theor. Biol. 105*, 403-425.
Langridge, R., & Ferrin, T. E. (1984) *J. Mol. Graphics 2*, 56.
Li, C. H. (1982) *Mol. Cell. Biochem. 46*, 31-41.
Marion, D., & Wüthrich, K. (1983) *Biochem. Biophys. Res. Commun. 113*, 967-974.
Merrifield, R. B. (1964) *J. Am. Chem. Soc. 86*, 304-305.
Richmond, T. J., & Richards, F. M. (1978) *J. Mol. Biol. 119*, 537-555.
Roeske, R. W., & Gesellchen, P. D. (1976) *Tetrahedron Lett. 38*, 3369-3372.
Sasaki, K., Dockerill, S., Adamiak, D. A., Tickle, I. J., & Blundell, T. (1975) *Nature (London) 257*, 751-757.
Schulz, G. E., & Schirmer, R. H. (1979) *Principles of Protein Structure*, Springer-Verlag, New York.
Shoemaker, K. R., Kim, P. S., York, E. J., Stewart, J. M., & Baldwin, R. L. (1987) *Nature (London) 326*, 563-567.
Stewart, J. M., & Young, J. D. (1969) *Solid Phase Peptide Synthesis*, Freeman, San Francisco, CA.
Taniuchi, H., & Anfinsen, C. B. (1969) *J. Biol. Chem. 244*, 3864-3875.
Theriault, Y., Boulanger, Y., Weber, P. L., & Reid, B. R. (1987) *Biopolymers 26*, 1075-1086.
Weiner, P. K., & Kollman, P. A. (1981) *J. Comput. Chem. 2*, 287.
Wüthrich, K. (1986) *NMR of Proteins and Nucleic Acids*, Wiley, New York.
Yang, J. J., Wu, C.-S. C., & Martinez, H. M. (1986) *Methods Enzymol. 130*, 208-269.
Zimm, B. H., & Bragg, J. K. (1959) *J. Chem. Phys. 31*, 526-535.

Use of EDTA Derivatization To Characterize Interactions between Oligodeoxyribonucleoside Methylphosphonates and Nucleic Acids†

Shwu-Bin Lin, Kathleen R. Blake, Paul S. Miller,* and Paul O. P. Ts'o
Division of Biophysics, School of Hygiene and Public Health, The Johns Hopkins University, Baltimore, Maryland 21205
Received June 20, 1988; Revised Manuscript Received September 14, 1988

ABSTRACT: EDTA-derivatized oligonucleoside methylphosphonates were prepared and used to characterize hybridization between the oligomers and single-stranded DNA or RNA. The melting temperatures of duplexes formed between an oligodeoxyribonucleotide 35-mer and complementary methylphosphonate 12-mers were 4-12 °C higher than those of duplexes formed by oligodeoxyribonucleotide 12-mers as determined by spectrophotometric measurements. Derivatization of the methylphosphonate oligomers with EDTA reduced the melting temperature by 5 °C. Methylphosphonate oligomer-nucleic acid complexes were stabilized by base stacking interactions between the terminal bases of the two oligomers binding to adjacent binding sites on the target. In the presence of Fe^{2+} and DTT, the EDTA-derivatized oligomers produce hydroxyl radicals that cause degradation of the sugar-phosphate backbone of both targeted DNA and RNA. Degradation occurs specifically in the region of the oligomer binding site and is approximately 20-fold more efficient for single-stranded DNA than for RNA. In comparison to the presence of one oligomer, the extent of target degradation was increased considerably by the additions of two oligomers that bind at adjacent sites on the target. For example, the extent of degradation of a single-stranded DNA 35-mer caused by two contiguously binding oligomers, one of which was derivatized by EDTA, was approximately 2 times greater than that caused by the EDTA-derivatized oligomer alone. Although EDTA-derivatized oligomers are stable for long periods of time in aqueous solution, they undergo rapid autodegradation in the presence of Fe^{2+} and DTT with half-lives of approximately 30 min. This autodegradation reaction renders the EDTA-derivatized oligomers unable to cause degradation of their complementary target nucleic acids. It appears that cleavage of the EDTA portion of the molecule by hydroxyl radicals is the major cause of this autodegradation and that the methylphosphonate backbone is resistant to cleavage.

Recently a class of "DNA affinity cleaving" molecules composed of a DNA binding molecule and a "molecular scissors" has been described (Schultz et al., 1982; Bowler et al., 1984; Chu & Orgel, 1985; Dreyer & Dervan, 1985; Doan et al., 1986, 1987; Chen et al., 1987; Sluka et al., 1987). This class of compounds is able to cleave DNA at the binding site of the DNA binding molecule. Such compounds have been used in footprinting experiments in place of the more tradi-

†This research was supported in part by grants from the National Institutes of Health (GM 31927) and the National Cancer Institute (Ca 42762).

0006-2960/89/0428-1054$01.50/0